Fuel 215 (2018) 865–878

Contents lists available at ScienceDirect

Fuel

journal homepage: www.elsevier.com/locate/fuel

Full Length Article

Conversion of petroleum coke into valuable products using oxy-cracking technique

Abdallah D. Manasrah, Nashaat N. Nassar*, Lante Carbognani Ortega

Department of Chemical and Petroleum Engineering, University of Calgary, 2500 University Drive NW, Calgary, Alberta T2N 1N4, Canada

GRAPHICAL ABSTRACT

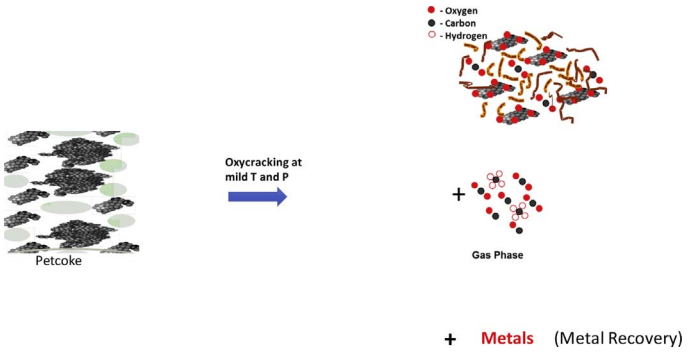

ARTICLE INFO

Keywords:
Oxy-cracking
Oxidation
Cracking
Petroleum coke
Solubility
Reaction kinetics
Demineralization

ABSTRACT

The global production of residual feedstock has reached 150 million metric tons per annum and is expected to increase in the future due to the progressively increasing heavier nature of the crudes. Petroleum coke (petcoke), one of these residues, is a solid-rich carbon typically produced during the upgrading of heavy oil and delay coking of vacuum residue in the refinery. Finding an alternative technique to treat this massive amount of petcoke is highly needed as the conventional processes like gasification and combustion have limitations in terms of efficiency and environmental friendliness. In this study, an oxy-cracking technique, which is a combination of cracking and oxidation reactions, is conducted as an alternative approach for petcoke utilization. The reaction is conducted in a Parr reactor where petcoke particles are solubilized in an aqueous alkaline medium and partially oxidized under mild operating temperature and pressure. Several operating conditions on petcoke oxy-cracking were investigated, such as temperature, oxygen pressure, reaction time, particle size and mixing rate to optimize the solubility and selectivity of oxy-cracked products. The results showed that the temperature and the residence time are the two major important parameters that affect the reaction conversion and selectivity. This enabled us to propose a reaction pathway based on the radical mechanism to describe the kinetic behavior of petcoke. Reaction kinetics indicated that petcoke oxidation undergoes a parallel-consecutive reaction in which an oxidative decomposition took place in the first step producing different oxidized intermediates. The oxy-cracked petcoke was characterized by FTIR, XPS and NMR analyses. The oxy-cracked products were found to contain carboxylic, carbonyl, phenolic, and sulfonic functions. Moreover, the elemental analysis showed that most of the metals remained in the residue, suggesting that the proposed technique could be employed for petcoke demineralization.

* Corresponding author.
E-mail address: nassar@ucalgary.ca (N.N. Nassar).

https://doi.org/10.1016/j.fuel.2017.11.103
Received 22 November 2017; Accepted 24 November 2017
Available online 22 December 2017

1. Introduction

Coking process is applied to upgrade bitumen, petroleum residue, vacuum residue, solvent-deasphalter pitch, rich asphaltenes and resin fuel, to more desirable products like LPG, naphtha, diesel and gas oil [1,2]. During the coking process, fuel gas and petroleum coke (petcoke) are also produced [3–5]. This coking process is typically a thermal cracking process in which the H/C atomic ratio of the product is increased by a carbon rejection mechanism [6]. Hence, multi-reactions that undergo a free radical mechanism are coupled together with cracking and polymerization reactions [7]. Cracking reactions produce gas and liquid products which are the most valuable ones, while radical polymerization reactions produce petcoke [8]. This petcoke is a rock-like structure mainly made out of carbon, hydrogen, nitrogen, sulfur and some metals. The global production of petcoke has reached about 150 million metric tons per annum. The North America alone produces about 70% out of the total petcoke capacity [9]. In 2014, Canada's oil sands reserves amounted to approximately 166 billion barrels, the third largest after Venezuela and Saudi Arabia [10,11]. In fact, in 2016, nearly 80 million tons of solid waste hydrocarbons (petcoke) were being stockpiled in Alberta as a by-product of the Canadian oil sands industries [9]. Consequently, approximately two-thirds of the produced petcoke have been accumulated and stored on-site for many years [12,13]. Due to limited markets and minimal use for this commodity, the stockpile is growing at a rate of about 4 million tons a year [14,15].

Petcoke is also generated in refineries through either delayed or fluid coking processes at high temperature and pressure. These coking processes are highly dependent upon their thermal treatments [4]. Delayed coking commonly occurs at a temperature range of 415–450 °C, whereas fluid coking uses higher temperatures ranging from 480 to 565 °C [8,16–18]. Generally, the produced petcoke has a high carbon content (80–85 wt%) consisting of polycyclic aromatic hydrocarbons with low hydrogen content. It is worth noting that petcoke has a lower amount of ash, moisture, and volatiles compared to coal [8]. However, it contains high amounts of sulfur (5–7 wt%) and vanadium (~700 ppm), which can severely impact human and animal health [19]. Additionally, dust emissions from petcoke piles impose a serious threat to people in the vicinity [19,20]. Furthermore, petcoke can be classified into calcined and green coke, where the latter is the initial product of the coking process that can be used as fuel in metallurgical and gasification processes [20]. Calcined coke, on the other hand, is produced by treating the green coke at a high temperature between 1200 and 1350 °C [20,21]. Depending upon its physical properties, structure, and morphology, the calcined coke can be formed as a sponge, shot and needle coke [22]. Oil sands companies often use different coking techniques [23]. Suncor Energy's coking process, for example, produces "delayed" petcoke, which has a sponge-like structure [24]. In contrast, Syncrude's coke is known as "fluid" coke and it has highly-graphitized layers and is often described to have an onion-like structure [23,25].

Petcoke has a high calorific value, as indicated from the literature at approximately ~37 MJ/kg, which makes it a valuable fuel resource for future application [26,27]. Therefore, alternative uses of this material could be considered and of paramount importance. Recently, a number of researchers have investigated the potential use of petcoke as a precursor for production of activated carbon due to its high carbon content [5,28,29]. Meanwhile, many studies have demonstrated that petcoke can be thermally, physically and chemically activated, in the presence of a reagent to produce activated carbon with the high specific surface area (~500–1500 m^2/g) [28,30–33]. However, the costs of generating activated carbon through either physical or chemical activation processes tend to be quite high, especially when the yield does not balance the generating costs, thus the total investment cost would be challenging for large-scale industries [34,35]. Moreover, the corrosive nature of the chemical activating agents has negative environmental impacts and often limits its application [32].

Alternative applications have included the use of petcoke for heat generation purposes, such as combustion and gasification [15,17,36]. Hence, petcoke could be an alternative fuel in power generation due to its higher heating value and lower price than coal. Although petcoke is a potential combustible as a fuel source, combustion process would invariably produce large quantities of sulfur dioxide (SO_2) [37]. Gasification process, on the other hand, was implemented to produce syngas and hydrogen at high temperatures (800–800 °C) and pressures (145–1450 psi) [36,38]. Although the gasification process captures more energy content, it is more capital intensive [39–42]. Additionally, gasification is not deemed to be a reliable technology for the treatment of these waste hydrocarbons, primarily due to the decline in current gas prices and the recent increase in shale gas production [43,44].

Despite all the attempts and processes that have been proposed in the industry to treat and reduce the amount of these waste hydrocarbons, a massive amount of petcoke is still present. Therefore, the development of an efficient and environmentally friendly technology is still a challenging and of paramount importance. Recently, our research group has introduced an oxy-cracking technique for converting heavy solid hydrocarbons into valuable products using a model residual feedstock exemplified by Quinolin-65 (Q-65) and n-C_7 asphaltenes [40,45]. This technique is a combination of oxidation and cracking reactions in an aqueous alkaline media is inspired by asphaltenes oxidation and ozonolysis studies [46–51]. Through the oxy-cracking process, a new reaction pathway is offered in an aqueous alkaline medium, at mild temperatures (170–230 °C) and pressures (500–750 psi). Importantly, the oxy-cracking process has a high efficiency to convert the solid waste hydrocarbons into valuable light commodity products [40,45]. The oxy-cracked materials (i.e., not completely oxidized) become soluble in water via oxygen incorporation due to the polar functionalization of the aromatic edges and paraffinic terminal carbons. Hence, the oxy-cracking undergoes a parallel-consecutive reaction in which an oxidative decomposition took place in the first step producing different aromatic intermediates. Those intermediates could be carboxylic acids and their corresponding salts, or other products [45,52,53]. Because of the high solubility and selectivity of oxy-cracked products in the alkaline medium and the insignificant amount of produced CO_2, the oxy-cracking process could be considered an environmentally friendly one. Similarly, a theoretical and experimental study on oxy-cracking of the Quinolin-65 (Q-65) molecule as a model molecule for residual feedstocks has recently confirmed that the attacks of the hydroxyl radical (·OH) plays an important role in the oxy-cracking reaction of Q-65 and n-C_7 asphaltenes [40,45].

Herein, in this study, we are applying the oxy-cracking technique as a new approach for converting petcoke into valuable commodity products by solubilizing it in water under alkaline conditions. The maximum solubilization and selectivity of oxy-cracked petcoke (i.e., desired products) in alkaline media with minimal emission of CO_2 are the main target. Eventually, at the end of the reaction, the oxy-cracked products are characterized using Fourier transformed infrared spectroscopy (FTIR), total organic carbon analysis (TOC), nuclear magnetic resonance (NMR) spectroscopy, and X-ray photoelectron spectroscopy (XPS) techniques. The gas emissions generated during the oxy-cracking process are also idintifed using gas chromatography (GC). The non-reacted solid residue is also analyzed using elemental analysis and FTIR as well. Moreover, the generalized "triangular" lumped kinetic model [54] is used here to determine the reaction kinetics parameters and the potential mechanism for the oxy-cracking of petcoke. It is expected that this study opens a better outlook about the use of the oxy-cracking process in the oil industry, mainly in treating residual feedstock such as petcoke and the like.

Table 1
The chemical composition of the green petcoke sample considered in this study.

Composition	C	H	N	S	V	Fe	Ni	Mo	Co	O*
wt%	84.48	3.81	1.55	4.46	0.08	0.06	0.03	0.01	0.15	5.37

* Estimated by difference.

2. Experimental work

2.1. Materials

A sample of green petcoke was obtained from Marathon Petroleum Company (Garyville, USA). This black-solid sample has complex hydrocarbons structure which consists of polycyclic aromatic hydrocarbons (3–7 ring), such as benzopyrene. The sample was grinded and sieved to the particle size ranging between 53 and 710 μm. The elemental analysis for the petcoke sample was carried out using a PerkinElmer 2400 CHN analyzer (Waltham, Massachusetts, USA) for C, H, N contents and a Thermo Intrepid inductively coupled plasma-atomic emission spectroscopy (ICP-AES) for sulfur and metal contents. The chemical composition of the selected petcoke sample is listed in Table 1.

KOH (ACS reagent, ≥85%, pellets form) purchased from Sigma-Aldrich (Ontario, Canada) was used to adjust the pH of the reaction medium (deionized water) and help in solubilizing the petcoke in water. Oxygen 99.9% ultrahigh purity purchased from Praxair (Calgary, Canada) was used as the oxidant gas.

2.2. Experimental procedures and setup

Fig. 1 shows a schematic representation of the experimental setup. The setup consists of a 100 mL reactor vessel (model number 4598, Parr Instrumental Company, Moline, Il, USA). The reactor vessel is made of stainless steel SS-316 with 12 cm in length and 3.25 cm in diameter. The vessel was equipped with a heating oven connected to a temperature control loop, a pressure gauge and a mechanical stirrer with a speed controller. The reactor vessel is capable of handling pressures up to 1700 psi and temperatures up to 270 °C. The oxy-cracking experiments were carried out at temperatures from 150 to 250 °C and pressures up to 1000 psi. In a typical experiment, 1.0 g of solid petcoke sample was charged into the reactor vessel containing 20 g of deionized water and a specified amount of KOH. The pH of the reaction medium is kept above 8.0 by adding 1.0 g KOH to assist in solubilizing petcoke and to avoid corrosion problems. Leak tests were performed by pressurizing the reactor with O_2 up to 1200 psi prior to fixing the operating pressure. Then, the mixer was set to 1000 rpm to minimize the interfacial mass resistance between the gas and liquid phase and to ensure uniform temperature and concentration profiles in the liquid phase. The reactor was then heated to the desired temperature. Once the desired pressure and temperature are attained, the zero-reaction time was considered. The reaction was carried out at different residence times, namely 15, 30, 45, 60, 120, 180 and 240 min. Several operating parameters were investigated to optimize the oxy-cracking reaction, such as temperature, reaction time, oxygen pressure, mixing speed, particle size and amount of KOH. At the end of the reaction, the reactor was cooled down to room temperature. Then, the gas phase was analyzed using gas chromatography, GC (SRI 8610C, SRI Instruments). Afterwards, the liquid effluents were carefully discharged and filtered for total organic carbon (TOC) analysis. A small amount of presumably unreacted solid residue was collected at the bottom of the reactor vessel. The oxy-cracked and insolubilized (residual) petcoke were recovered using an evaporator (vacuum oven) for further analysis by Fourier transformed infrared spectroscopy (FTIR), nuclear magnetic resonance (NMR) spectroscopy and X-ray photoelectron spectroscopy (XPS) to investigate the nature of the formed compounds. Also, elemental analysis was performed on the dried recovered solids.

2.3. Characterization

2.3.1. FTIR analysis

The chemical structure of the virgin petcoke sample, oxy-cracked (solubilized) and insoluble solid (residue) were characterized with a Shimadzu IRAffinity-1S FTIR (Mandel, USA), provided with a smart diffuse reflectance attachment to carry out diffuse reflectance infrared Fourier transform spectroscopy (DRIFTS) analysis. Initially, the background was defined by analyzing about 500 mg of pure potassium

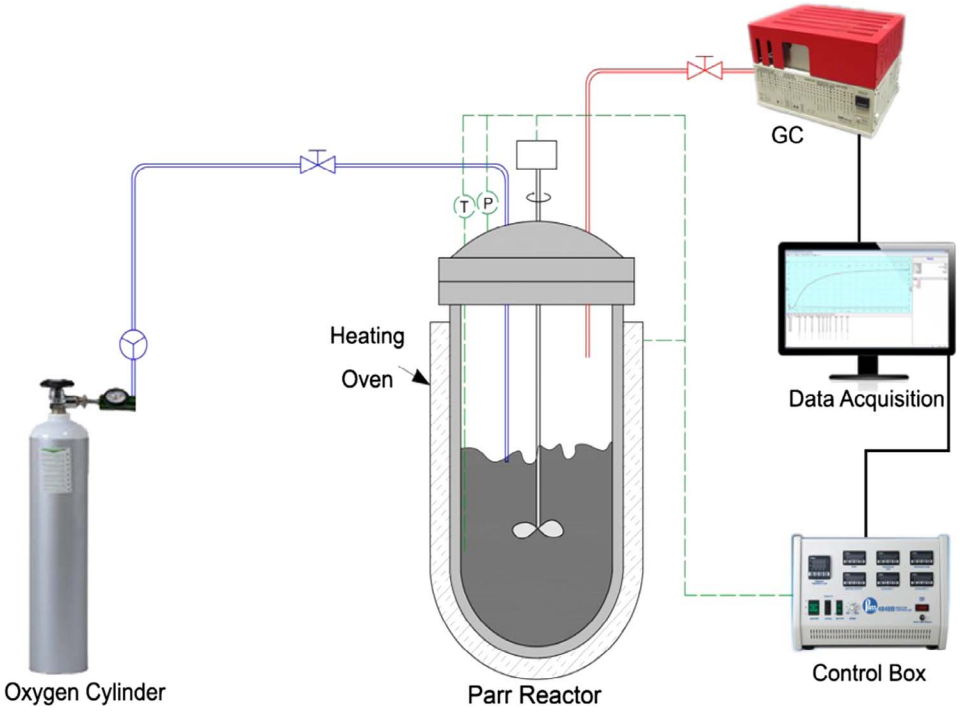

Fig. 1. Schematic representation of the experimental setup (not to scale).

bromide (KBr) powder; then, approximately 5 mg of the petcoke sample dispersed in the 500 mg of KBr was analyzed. The IR spectra were obtained in the wave number ranging from 400 to 4000 cm^{-1}; all the spectra were acquired as averages of 50 scans with a resolution of 4 cm^{-1}. It is worth noting here, in case of oxy-cracked (solubilized) sample, the solidified organic species were collected by drying the solubilized petcoke in water overnight at 65 °C in a vacuum oven.

2.3.2. Total organic carbon (TOC) analysis

A Shimadzu total organic carbon analyzer (TOC-L CPH/CPN) was used to determine the carbon content of the solubilized organic and inorganic species present in the water. The TOC samples were prepared by centrifuging the solubilized species in a centrifuge (Eppendorf centrifuge 5804) at 5000 rpm and 15 min to separate the remaining solid (i.e., unreacted and insolubilized species). The total carbon (TC), total organic carbon (TOC), and inorganic carbon (IC) of the aqueous phase were measured. Both TC and IC measurements were calibrated using standard solutions of potassium hydrogen phthalate and sodium hydrogen carbonate. Fifteen milliliters of the centrifuged solutions were placed in standard TOC vails. Using the TOC software to control the system, the TC was automatically measured. After that, an acid was added to evolve CO_2 from the sample to measure the remaining organic compounds, which were considered as TOC. All the measurements were taken three times, and the average was used for the calculations with a 5% relative standard deviation.

2.3.3. ^1H nuclear magnetic resonance (NMR) spectroscopy

The NMR spectrum of the oxy-cracked sample was determined with a Bruker 600 MHz spectrometer (4 mm BL4 liquid probe, cross-polarization program, and spin rate of 8 k). The ^1H NMR spectrum was taken at 298 K using a D_2O solvent with a pulse sequence zg30, a relaxation time of 2 s, and averaging 160 scans/run. The NMR spectrum was analyzed using the commercial NMR simulator software (Mnova NMR) helping the assignment of most structure types available at different frequencies.

2.3.4. Gas chromatography (GC) analysis

The compositional analysis of the produced gases was carried out with a GC (SRI 8610C Multiple Gas #3 gas chromatograph SRI Instruments, Torrance, CA). The GC was provided with a thermal conductivity detector (TCD) and two packed columns connected in parallel (3′ molecular sieve/6′ Hayesep-D columns). The molecular sieve column is used for permanent gases, while the Hayesep-D column allows analysis for hydrocarbons up to C5. The gas analysis was carried out after the oxy-cracking reaction is completed and cooled down to room temperature. The GC measurements were repeated 5 times for each sample, and the average relative error was lower than 3%.

2.3.5. X-ray photoelectron spectroscopy (XPS)

The XPS analysis was conducted on the petcoke sample before and after reaction using an XPS PHI VersaProbe 5000 spectrometer to provide information about the distribution of different atoms on the sample surface based on their binding energy. The oxy-cracked sample was collected after drying it in a vacuum oven at 65 °C overnight. XPS spectra give an additional information about the nature of bonds and component analysis [55]. The spectra were taken using a monochromatic Al source (1486.6 eV) at 50 W and a beam diameter of 200.0 μm with a take off angle of 45°. The samples were pressed on double-sided tape and the spectra were taken with double neutralization. The sample sputtering protocol involved 20 min of Argon sputtering at 45°, 2 kV, 1.5 μA 2 × 2 (less than 10.5 nm/min). Calibration was performed with a SiO_2/Si wafer having a SiO_2 layer of 100 nm.

2.3.6. Elemental analysis

A combustion method using a PerkinElmer 2400 CHN analyzer (Waltham, Massachusetts, USA) was used for analyzing carbon, hydrogen, and nitrogen contents after and before oxy-cracking reaction. Both sulfur and nitrogen contents for organic materials were determined with an Antek 9000 system (Houston, TX, USA) by running toluene solutions (10 wt%/vol.). Calibration was performed with Accustandard IS-17368 (N) and Accustandard SCO-500x (S) standards.

For metal analysis (Fe, Ni, Co, Mo and V), the microwave assisted acid digestion procedure was used in a commercial unit model MARS 6 from CEM Corporation (Matthews, NC, USA) for digesting the solid residual samples. The system is provided with UltraPrep vessels of 100 mL capacity and a MARSXpress DuoTemp controller which was operated at a frequency of 2.45 GHz at 100% of full power (maximum of 1600 W). Sulfur and metal concentrations in the oxy-cracked and residual samples were determined by ICP–AES.

3. Results and discussion

3.1. Reaction kinetics

The oxy-cracking reaction mechanism of heavy hydrocarbon compounds is very complex. Even with a pure compound such as phenol, the high-temperature wet oxidation exact mechanism or reaction pathway has not been established yet [54,56]. The wet oxidation of hydrocarbon mixtures is much more complex than a single compound. Based on our recent findings on the oxy-cracking of model hydrocarbon compounds (Q-65), it was observed that the compound underwent a consecutive reaction in which an oxidative decomposition takes place in the first step producing different aromatic intermediates [45,57]. The intermediates were oxy-cracked consecutively into different families of organic acids and small amounts of solubilized CO_2 [56]. Similar reaction pathway has been proposed for oxy-cracking of n-C_7 asphaltenes [40]. Using oxygen as an oxidizing agent, the asphaltenes was oxygenated and functionalized to different families of carboxylic, sulfonic, and phenolic compounds. This mechanism is inspired by the generalized kinetic model for wet air oxidation of organic compounds existing in wastewater which was proposed by Li et al. [54]. Accordingly, the oxy-cracking mechanism of petcoke is believed to obey similarly the triangular reaction pathway, as depicted in Fig. 2, where petcoke slowly solubilized in water with small quantities of produced CO_2 at early stages of the reaction. Under certain reaction conditions, longer residence time and higher temperature, the solubilized petcoke in water starts reacting with oxygen to produce CO_2.

Considering the petcoke has a complex structure [58–60], many soluble and insoluble intermediates were produced during the reaction. The concentration of the intermediates (desired products) in the liquid phase was calculated based on carbon mass as the lumped total organic carbon (TOC) concentrations. However, the carbon content of initial feedstock was calculated using elemental analysis; carbon content before reaction (feedstock) = (mass of petcoke) × (carbon% in feed). The produced gas, most likely CO_2, was analyzed online using GC. Other determined gas concentrations were very small, thus neglected. The reaction conversion based on carbon mass was calculated based on the following equation,

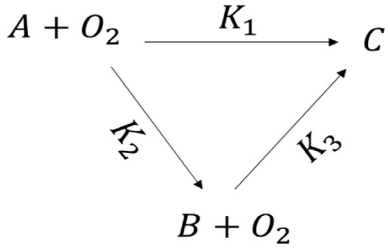

Fig. 2. Triangular reaction scheme of petcoke oxy-cracking, where A is the petcoke, B is the intermediates (desired products, TOC), and C: CO_2 in the gas phase (C_G) + CO_2 in the liquid phase (carbonates IC).

$$\text{Conversion,X} = \frac{C_{A0} - C_R}{C_{A0}} \quad (1)$$

where C_{A0} is the carbon concentration of virgin petcoke before the reaction, C_R is the residual carbon concentration (unreacted petcoke) that remains after the reaction. It is worth noting that the numerator term ($C_{A0}-C_R$) in Eq. (1) represents the amount of carbon in the liquid phase as total carbon ($TC = TOC + IC$) and the amount of carbon in the gas phase CO_2 (C_G). Hence,

$$C_{A0} - C_R = (TOC) + (IC) + C_G \quad (2)$$

considering the CO_2 gas obeys the ideal gas behavior, then the carbon content in the gas phase (C_G) could be calculated as follows;

$$C_G = 12 \times \frac{PV}{RT} \quad (3)$$

where P and T are the pressure and temperature at the end of reaction, respectively. V is the volume of the gas phase in the reactor vessel and R is the ideal gas constant.

The selectivity to produce the desired products (B) and CO_2 (C) was calculated as follow,

$$\text{Selectivity to product B} = \frac{(TOC)}{(TOC) + IC + C_G} \quad (4)$$

$$\text{Selectivity to product C} = \frac{(IC + C_G)}{(TOC) + IC + C_G} \quad (5)$$

The kinetic rate equations for the oxy-cracking reaction in a batch reactor, as shown in Fig. 2, can be expressed by the set of the following three differential equations:

$$\frac{dC_A}{dt} = -r_A = (K_1 + K_2)C_A^{n1} \quad (6)$$

$$\frac{dC_B}{dt} = +r_B = K_2C_A^{n1} - K_3C_B^{n2} \quad (7)$$

$$\frac{dC_C}{dt} = +r_C = K_1C_A^{n1} + K_3C_B^{n2} \quad (8)$$

where,

$$K_1 = k_1' e^{-E_1/RT} C_{O_2}^m \quad (9)$$

$$K_2 = k_2' e^{-E_2/RT} C_{O_2}^m \quad (10)$$

$$K_3 = k_3' e^{-E_3/RT} C_{O_2}^m \quad (11)$$

where C_A, C_B, and C_C are the carbon concentrations of original petcoke, intermediate (desired products), and CO_2, respectively. C_{O2} is the concentration of oxygen, n1,n2 and m are the reaction order of A, B and O_2, respectively. t is the reaction time, and K_1, K_2, and K_3 are the reaction rate constants.

The reaction orders are experimentally determined to be first order for A and B, i.e., n1 = n2 = 1. Typically, the order of oxygen is either near zero ($m = 0$) or excess oxygen is used to reduce its effect on the reaction kinetics and enable hydrocarbon species (A and B) to be the limiting reactant [54,61,62]. Therefore, the oxygen terms will be considered as a constant, hence, Eqs. (6)-(8) can be expressed as follows:

$$\frac{dC_A}{dt} = -(K_1 + K_2)C_A \quad (12)$$

$$\frac{dC_B}{dt} = K_2C_A - K_3C_B \quad (13)$$

$$\frac{dC_C}{dt} = K_1C_A + K_3C_B \quad (14)$$

The kinetic parameters, i.e., K_1, K_2, and K_3 were estimated using the Mathematica software (V10.2) by fitting the experimental data to the differential equations (12)–(14) under the following initial conditions: at t= 0, $C_A = C_{Ao}$, and $C_B = C_C = 0$. The proportional weighed sum-of-squares was minimized using the Mathematica until all values of the correlation coefficient (R^2) were very close to 1.0. The kinetics experimental data were collected at three different temperatures of 200, 215, and 230 °C and reaction times varying from 0 to 1 h. However, other important parameters, such as the operating partial pressure (750 psi), the mass ratio of petcoke to KOH, and the impeller speed (1000 rpm) were all kept fixed. At these temperatures and reaction times, the best range of conditions was selected to make the reaction favorable to the desired products. Indeed, at high temperatures (> 250 °C) and residence times (> 2 h), combustion reaction becomes more favorable than oxy-cracking and more CO_2 was produced. However, low reaction conversions were obtained at low temperatures (< 180 °C). The oxy-cracking reaction was not significantly affected by the oxygen partial pressure beyond 750 psi. Also, the oxy-cracking reaction rate was found to be independent of the impeller speed above 500 rpm, indicating there is no mass transfer limitation beyond this speed limit. These constrains and findings were acknowledged in the literature for oxy-cracking and wet air oxidation of hydrocarbon compounds [40,43,45,52,53,63,64].

The estimated reaction constants of the petcoke oxy-cracking are presented in Table 2. Consequently, the activation energies and frequency factors were estimated using Arrhenius equation based on the temperature and reaction constants as follow:

$$K_i = k_i' e^{\frac{-E_i}{RT}} \quad (15)$$

where k_i' is the frequency factor for each step of the reaction, E_i is the activation energy, i is the reaction step pathway (1, 2, and 3), R is the ideal gas constant, and T is the temperature.

Fig. 3 compares the experimental data with the kinetic model for concentration profiles of petcoke (A), intermediate compounds (B), and CO_2 (C) at three different temperatures of 200, 215, and 230 °C as a function of time. Noticeably, the kinetic model showed an excellent agreement with the experimental results and described the proposed triangular reaction kinetics scheme accurately. It is clear that the reaction temperature is acting as a key parameter in the oxy-cracking reaction. Thus, at a higher temperature (i.e., 230 °C), the solubilization of oxy-cracked compounds in water is increased and reached to the maximum concentration faster than at lower temperatures. Moreover, at a high reaction temperature, the produced CO_2 in the gas phase is detected at the early stage of the reaction. Even at low reaction time, i.e., 15 min, the amount of produced CO_2 is determinable by GC. This indicates that a direct reaction might be occurring between oxygen and petcoke to form CO_2. These findings line up perfectly with our previous works on oxy-cracking of model compounds (Q-65) and asphaltenes [40,45].

Fig. 4 represents the Arrhenius plot of petcoke oxy-cracking reaction at three different reaction temperatures. By plotting ln(k) against 1/T, a good fitting was accomplished between Arrhenius equation and the experimental data, indicated by R^2 values closed to 1. From the slope and intercept of the best-fit-line at each temperature, the values of activation energies and frequency factors of petcoke oxy-cracking were calculated and summarized in Table 3.

Moreover, the experimental and theoretical findings in our previous works on oxy-cracking [45] and thermo-oxidative decomposition [65] of Q-65 as a model molecule of heavy solid hydrocarbons confirmed that the reaction initiates by cracking the weakest bond in the alkyl

Table 2
Determined values of oxy-cracking reaction constants.

T (°C)	K_1 s^{-1}	K_2 s^{-1}	K_3 s^{-1}
200	2.27×10^{-5}	1.84×10^{-4}	1.71×10^{-5}
215	6.99×10^{-5}	3.46×10^{-4}	2.42×10^{-5}
230	2.43×10^{-4}	87.37×10^{-4}	3.67×10^{-5}

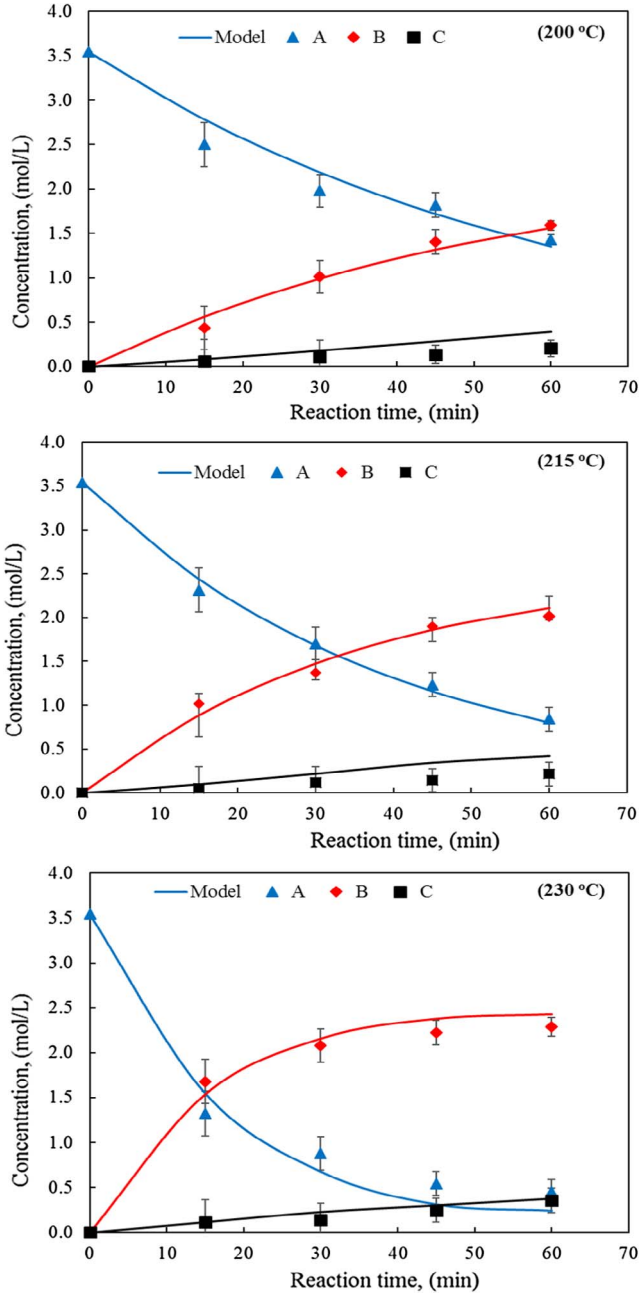

Fig. 3. Concentrations of A, B, and C as a function of reaction time at different reaction temperature 200 °C, 215 °C, and 230 °C. The symbols represent experimental data, and the solid lines are the kinetics model (Eqs. (12)-(14)).

chain to produce CO_2. However, in case of Q-65 oxy-cracking reaction, after the alkyl chain initially cracked using hydroxyl radical (˙OH), the dissociation of the carbon bonds adjacent sulfur is consequently taken place. After that, the whole molecule is completely cracked to produce phenolic and carboxylic substances and a small amount of CO_2. Accordingly, similar reaction mechanism and pathways could be considered here for the case of petcoke oxy-cracking. Hence, at the beginning of the reaction, an induction period is found in which there is small amount of CO_2 released. The reason of that refers to the oxygen which is initially incorporated into the petcoke/hydrocarbons molecules, after that a complete release of CO_2 takes place. Nevertheless, this small amount of CO_2 was noticed due to the short alkyl chains that present in the petcoke structures as confirmed in the FTIR results. This finding also supported by the highest value of activation energy (E_1 = 165.12 kJ/mol) in the first reaction pathway. Additionally, the

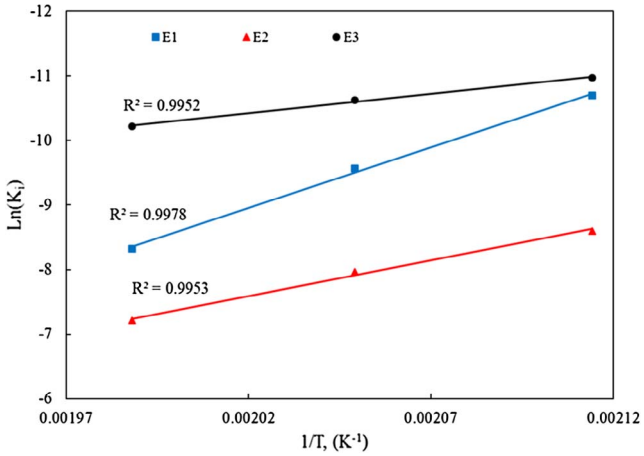

Fig. 4. Arrhenius plots of petcoke oxy-cracking for each reaction pathway.

Table 3
Estimated activation energies and frequency factors of petcoke oxy-cracking.

Activation energy (kJ mol^{-1})		Frequency factor (s^{-1})
E_1	156.12	1.74×10^{12}
E_2	91.50	2.19×10^{6}
E_3	50.12	5.75

value of activation energy could be attributed to the complexity of aggregated structures of petcoke molecules [66–68]. Subsequently, petcoke aggregates require more oxygen penetration during the oxy-cracking reaction to achieve the desired conversion. Even though petcoke is not completely dissolved in water at the beginning of the reaction, their nature is changed during the reaction due to the presence of KOH and partial oxidation. Therefore, petcoke particles were solubilized in water as oxygenated hydrocarbons analogs of carboxylic acids and the like. These findings were confirmed in the second reaction pathway where the activation energy E_2 = 91.50 kJ/mol and a high value of the frequency factor 2.19×10^6 s^{-1}. Consequently, CO_2 could be produced in the third reaction pathway, E_3 = 50.12 kJ/mol, by further reaction between solubilized aromatic moieties and oxygen. Although the activation energy for deep oxidation of petcoke to produce CO_2 in the first reaction pathway (165.12 kJ/mol) is much higher than the one obtained in the third pathway (partial oxidation) (50.12 kJ/mol), the frequency factor in the first pathway (1.74×10^{12} s^{-1}) is also higher than the third pathway (5.75 s^{-1}). These findings also support that the rate consuming of petcoke into CO_2 at the beginning of reaction could happen at the same rate of CO_2 production from the oxidation of the organic compounds solubilized in water. In other words, the rate of forming and producing intermediate compounds (desired products) is more favorable than producing CO_2 in both reaction pathways, as the activation energy (E_2) was lower than E_1 and the frequency factor (k'_2) is higher than k'_3. Similar trends were reported for oxy-cracking of model hydrocarbons Q-65 [45] and n-C_7 asphaltenes [40].

3.2. Effects of operating conditions on petcoke oxy-cracking reaction

In this section, the effects of operating conditions such as temperature, residence time, oxygen partial pressure, amount of KOH, petcoke particle size and impeller speed were investigated. These parameters were optimized not only to maximize the reaction conversion and selectivity to produce the water-solubilized hydrocarbons (desired products) but also to minimize the amount of CO_2 produced during the oxy-cracking reaction. Preliminary experiments were conducted to optimize the operating oxygen partial pressure. The results revealed that the reaction conversion was not significantly affected by

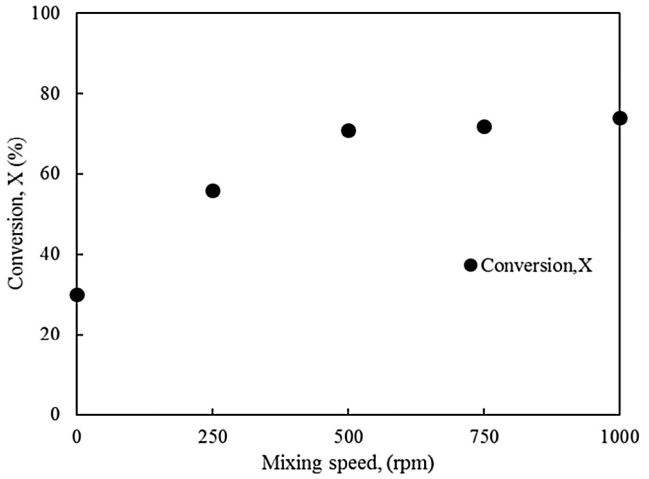

Fig. 5. Effect of mixing speed on the conversion of petcoke during oxy-cracking reaction (T = 215 °C, P = 750 psi and t = 2 h).

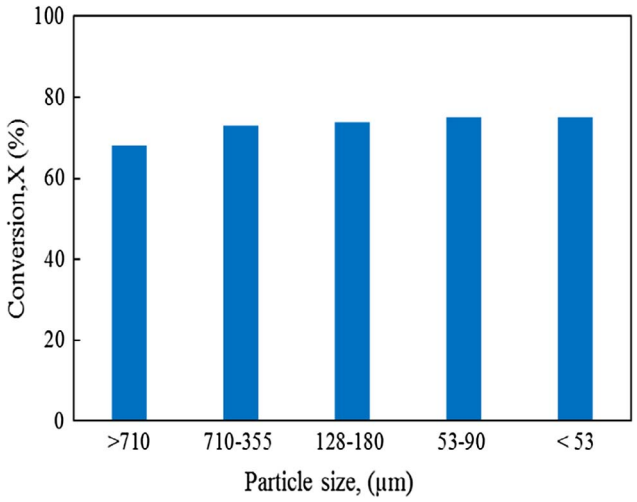

Fig. 6. Effect of petcoke particle size on reaction conversion of petcoke (T = 215 °C, P = 750 psi and t = 2 h).

oxygen partial pressure beyond 750 psi. Therefore, at this pressure and temperature range (180–230 °C), the water exists only as a subcritical liquid. It is worth noting here that the oxygen is not utilized only in converting the petcoke to CO_2 and water, but also a good proportion of oxygen is consumed in converting petcoke to water-soluble materials. Hence, at the given pressure, we ensured that oxygen is present in an excess amount.

The effect of mixing was investigated during the petcoke oxy-cracking reaction. High mixing speed should minimize the interfacial mass resistance between the gas and liquid phase, therefore enhancing the oxygen to transfer from the gas phase to the liquid phase. Additionally, the mixing speed helps to maintain a relatively uniform temperature and concentration profiles in the liquid phase [69–71]. The reaction conversion was evaluated by varying the mixing speed from 0 to 1000 rpm while fixing other parameters such as temperature (215 °C), oxygen pressure (750 psi) and reaction time (2 h). As seen in Fig. 5, it is clear that when the mixing speed is below 500 rpm, a significant reduction in the reaction conversion occurred, thus the mass transfer region considered to be the controlling step. However, above 500 rpm, the effect is drastically reduced and there was no practically effect on the reaction conversion, i.e., the reaction region is the controlling step. Therefore, a high mixing speed would result advantageous for the aqueous phase by providing a well-mixed reactor content during the reaction. Thus, to avoid the mass transfer resistance the reaction was taking place in the turbulent region (i.e., Reynolds numbers, Re > 10,000).

The effects of petcoke particle sizes were also investigated on the conversion of oxy-cracking reaction. Different petcoke particle sizes ranging from 53 to 710 μm were tested to examine their effect on petcoke solubilization or any mass transfer limitations. Fig. 6 shows the reaction conversion of petcoke oxy-cracking evaluated at different petcoke particle sizes, constant temperature (215 °C), mixing speed (1000 rpm), oxygen pressure (750 psi) and reaction time (2 h). As expected, no remarkable effect of particle size on the solubilization of petcoke can be seen. This suggests that the mass transfer has a relatively minor impact on the studied range of particle sizes. Within average, the total petcoke conversion to desired products and CO_2 was approximately constant (about 78.5%), and independent of particle size. These findings are valuable because grinding and manipulating very small particle sizes of petcoke are challenging and quite costly. Therefore, the obtained results have relevance for the possible implementation of the process at large scale.

3.2.1. Effect of the temperature

The effect of the temperature on the conversion and selectively of the oxy-cracking reaction was investigated between 180 and 250 °C. Other important parameters such as the oxygen partial pressure was set to 750 psi to make sure the water was present in the subcritical state, mixing rate was 1000 rpm to prevent the liquid phase interfacial mass transfer resistance, and the residence time was 1 h. Based on the reaction kinetic results, the reaction performance improved by increasing the temperature. In fact, the reaction temperature is a key parameter in the oxy-cracking reaction. Thus, by increasing temperature (i.e., up to 250 °C) the solubilization of oxy-cracked compounds in water is increased. Although the solubilization of oxygenated hydrocarbons is increased at a high temperature, the selectivity of producing CO_2 gas is also increased. Hence, under longer reaction times the oxygenated intermediates further decomposed oxidatively to CO_2 and H_2O. Furthermore, the chemical transformation of oxygenated intermediates to CO_2 appear to have complex mechanisms even at low reaction temperature.

Fig. 7 shows the conversion and selectivity of oxy-cracking reaction at different reaction temperatures. It is clear that as the temperature increased the petcoke conversion to produce solubilized-hydrocarbons (B) is increased with a slight increase in CO_2. However, the selectivity to produce the desired products (B) is slightly decreased with a further increase in temperature (250 °C). Moreover, no reaction occurred at temperatures lower than 150 °C with the considered residence time. For instance, the reaction conversion was less than 30% when the temperature ranged from 150 to 180 °C at 1 h residence time. Interestingly,

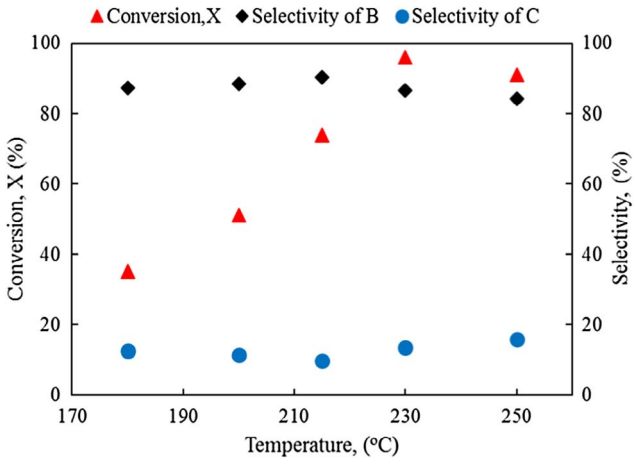

Fig. 7. Effect of the reaction temperature on the selectivity and conversion of petcoke oxy-cracking (P = 750 psi and t = 1 h).

the highest conversion was obtained when the temperature ranged from 220 to 240 °C. Based on that, the optimum reaction temperature which provides the highest conversion and selectivity to B synchronized with a minimal amount of CO_2 centers around 230 °C, as presented in Fig. 7.

The results showed that the temperature has a great effect on the conversion and less effect on the selectivity to water solubilized products. Nevertheless, the oxy-cracking temperature is a key parameter not only on the conversion and the selectivity but also on the acidity of formed products. Even the reaction rates are increased with temperature, the final TOC values of the desired products (B) for temperature higher than 230 °C are practically constant after 1 h. The reason of that is due to the ability of the low-molecular weight chemical species that resist the oxidation process. Another reason for this observation is the short life of free radicals (scavenging effects) since the presence of high strength carbonate buffer (KOH) might kill some of the free radicals which otherwise directly attack the other organic compounds as will be discussed in Section 3.2.3. Moreover, when the temperature is lower than 200 °C, the aqueous phase has an excess amount of free KOH (i.e., pH > 10). However, more acidic functional groups were produced at higher temperatures (200–250 °C), and this is confirmed by lowering the values of pH for neutralization reactions to about 8.5. The pH reduction lines up perfectly with similar trends reported for n-C_7 asphaltenes oxy-cracking [40,52] and oxidizing organic compounds in subcritical water such as phenols, benzene, and other alcohols [71,72].

3.2.2. Effect of reaction times

The effect of reaction time was also studied by varying the time from 15 min to 4 h under a constant pressure (750 psi), mixing speed (1000 rpm) and operating temperature of 180 °C. The effect of reaction time on the conversion and selectivity of oxy-cracking reaction is shown in Fig. 8. It is clear that the reaction conversion of petcoke to produce oxy-cracked hydrocarbons (B) and CO_2 is significantly increased with time. However, the selectivity to product B is slightly decreased with further increase in time, and simultaneously the selectivity to product C slightly increased with time. The optimum reaction time could be considered when the conversion and selectivity of B are high which was at time 2 h. Moreover, the effect of reaction time on the acidity of formed products has been noticed. By increasing the reaction time, the pH of the liquid phase decreased, thus more acidic compounds were produced.

3.2.3. Effect of KOH

The oxy-cracking reaction was studied by changing the dosage of KOH from 0 to 2.5 g at constant temperature (230 °C), oxygen pressure (750 psi), reaction time (2 h) and mixing speed (1000 rpm). Fig. 9 shows the effect of KOH on the reaction conversion and selectivity to both B and C. As seen, the conversion as well as the selectivity to B, significantly increased by increasing the amount of KOH and then slightly decreased by further increase of KOH dosage. However, the selectivity to C decreased by increasing the KOH amount. Thus, the optimal amount of KOH was chosen to be (1 g KOH/1 g petcoke) where the highest values of the reaction conversion and selectivity to B were achieved and the lowest amount of CO_2 was produced. In fact, KOH was needed here to prevent the corrosion effect caused by the high acidity species generated during the early oxidation stage of the process. The results showed that the KOH is also a key parameter for enhancing the solubilization of oxy-cracked materials, therefore increasing the reaction conversion, as well as the selectivity to the desired products. Some researchers [49,52,73] claimed that adding a base such as NaOH, KOH and NH_4OH might have a catalytic effect on water-solubilized materials by neutralizing the acidic species and/or displacing the saponification equilibrium. For example, naphthenic acids dissolve in hot water at basic conditions formed soluble organic salts [74]. These findings have been confirmed by other studies [44,75,76] where the solubility of species containing oxygen increased in the basic media. Patil et al. [75] showed that the solubility of lignin in water increased in presence of NaOH. Likewise, Ashtari et al. [52] showed that the alkaline medium enhanced n-C_7 asphaltene oxy-cracking and its subsequent solubilization in water. In this regard, 1.0 g of KOH per 1.0 g of petcoke was considered as the optimum value for the oxy-cracking experiments.

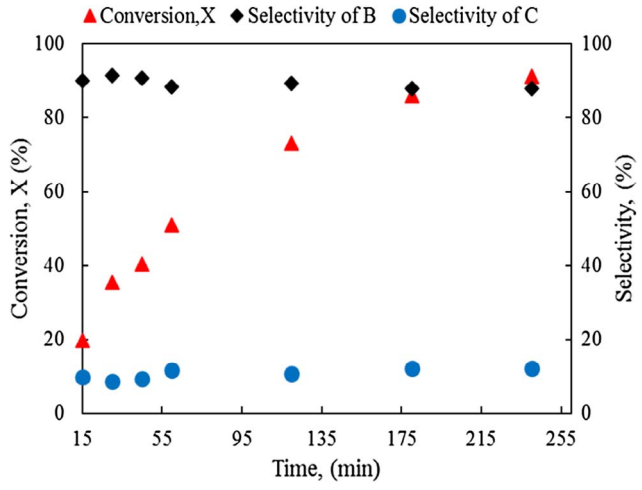

Fig. 8. Reaction time effect on selectivity and conversion of petcoke oxy-cracking reaction (T = 180 °C and P = 750 psi).

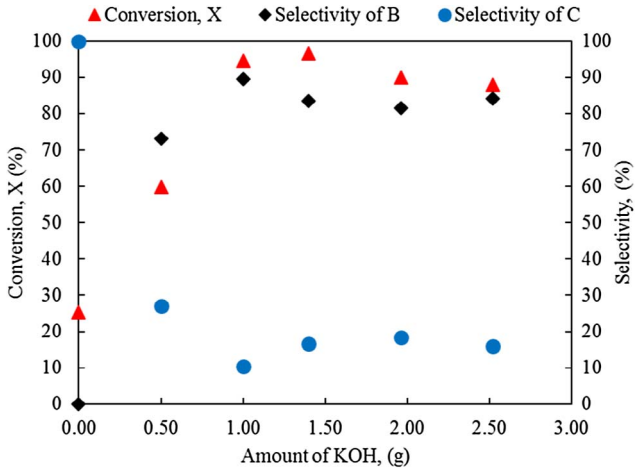

Fig. 9. Effect of KOH amounts on the selectivity and conversion of petcoke oxy-cracking reaction (T = 230 °C and P = 750 psi, time = 2 h).

3.3. Characterization results

3.3.1. FTIR analysis for petcoke and oxy-cracking products

FTIR analysis is one of the most versatile techniques to understand the structures of such complicated organic mixtures like petroleum coke and heavy hydrocarbons. This because FTIR has the ability to provide information about the functional groups based on their bond energies and orientation of atoms in space. The FTIR spectrum of the original petcoke was carried out and compared with the oxy-cracked product and the non-converted residue as well. Fig. 10 shows the infrared spectra of the original petcoke, residual petcoke (non-soluble solid) and oxy-cracked petcoke solubilized fraction isolated from the reaction carried out at 230 °C and 2 h (i.e., the optimum conditions). It is evident from the figure that FTIR spectra of original petcoke and the oxy-cracked one are distinctly different from each other.

The spectrum of the original petcoke shows IR bands that can be assigned to the alkyls/aliphatic (2850–3000 cm^{-1}) and aromatic (~3040 cm^{-1} and 930–750 cm^{-1}) regions. The presence of C—H bonds vibration out-of-plane in aromatics can be assigned to the 748, 804, and

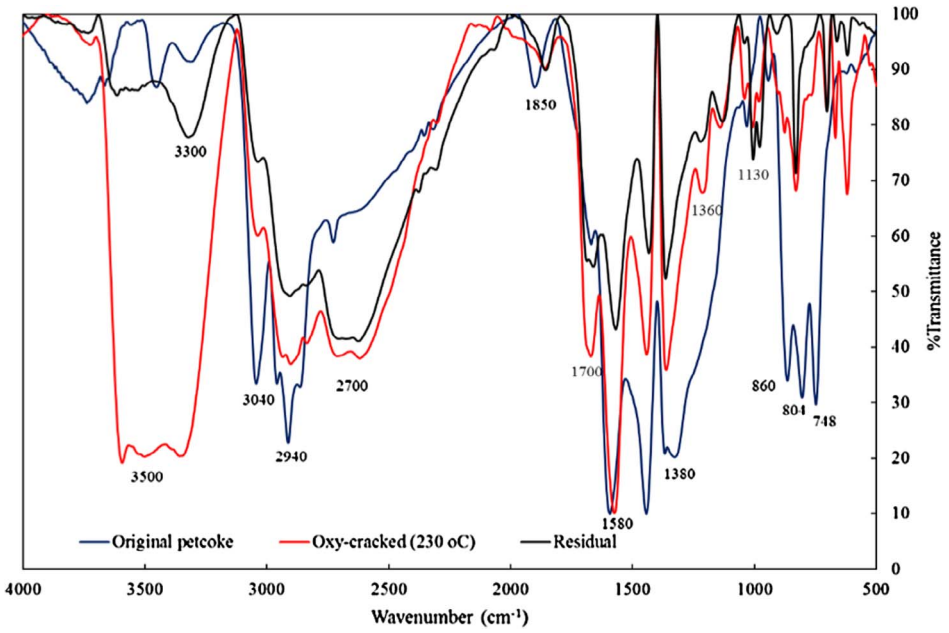

Fig. 10. FTIR spectra of the original petcoke, oxy-cracked products and residual petcoke at 230 °C and 2 h residence time.

860 cm^{-1} bands. The corresponding C═C aromatic stretching vibration appears near 1580 cm^{-1}, slightly below the typical 1600 frequency, thus believed conjugated with other groups like C = C region as reported in other studies [77–79]. However, for the oxy-cracked sample, the noticeable lower contribution from aromatic out plane bands is observed (930–750 cm^{-1}). The transmittance at 3040 cm^{-1} due to aromatic C—H stretching vibrations can be found in the spectra for both the original and the oxy-cracked petcoke; however, much less important in the later.

Furthermore, in the aliphatic region, the presence of alkyl groups in the petcoke sample such as $–CH_3$, $=CH_2$ and $–CH_2CH_3$ is evidenced by the bands around 2940 cm^{-1} and 1380 cm^{-1} which can be assigned to asymmetric and symmetric –C—H stretching and bending vibrations, respectively[80]. The weak band at around 3500 cm^{-1} observed for the original petcoke can be assigned to free O—H stretching vibration mode of hydroxyl functional groups. The broad-band spanning from about 2700 to 2000 cm^{-1} possibly corresponds to hydrogen bonded –OH functionalities. The presence of sulfoxide species in the original petcoke is assigned at the small band ~1031 cm^{-1}. These findings are in accordance with many studies reported by Pruski et al. [81] and Michel et al. [82] that showed the raw (green) petcoke comprises polynuclear aromatics with few alkyl chains as substituents and polynuclear aromatic molecules such as naphthalene, anthracene, benzo-pyrene, phenanthrene, coronene, triphenylene, and pyrene [67,83].

The FTIR spectrum of the insoluble petcoke (solid residue after reaction) is also appended in Fig. 10. Worth mentioning here that small amount of solid residue could only be collected at low reaction conversion for further characterizations. The structures of insolubilized solid material (residue) was found very similar to the original petcoke according to their IR spectra, with some features changed due to the contribution of oxygenated functions. It is clear from the spectrum that at 3300–3700 cm^{-1} there is a higher contribution of OH groups in the remaining insolubilized solid compared with the original petcoke. Also, the C—O—C contributions (1363 cm^{-1}) in the remaining solids was found less intense compared to the original petcoke which showed a broad-band spanning from about 1360–1100 cm^{-1}. This later band can also be derived from the contribution of sulfones (centered in 1130 cm^{-1}), in addition to other S-oxidized forms (sulfoxide at 1030 cm^{-1}) with higher intensity compared with the original and oxy-cracked samples.

The FTIR spectrum of the oxy-cracked petcoke is dramatically different from that of raw petcoke (Fig. 10). It is worth noticing that a new significant band, appearing as an intense and broad peak in the range between 3300 and 3600 cm^{-1} corresponds to —O—H stretching vibration mode of hydroxyl functional groups [84]. This might be explained due to the presence of oxygen in the aqueous phase, thus the organic species of petcoke are oxy-cracked to oxygenated species bearing alcoholic, carboxylic and phenolic functional groups. Interestingly, the presence of carboxylate anion is observed as a doublet band centered at 1500 cm^{-1}, indicating the presence of carboxylic salts. Free acids presence is also evidenced by the C═O band appearing at 1700 cm^{-1}, thus some of the –OH observed in 3300–3600 cm^{-1} can be assigned to these free acids. Another important feature is the disappearance of most aromatic moieties in the region of out-of-plane bands (930–750 cm^{-1}), together with the important reduction of the aromatic C—H stretching at 3030 cm^{-1}. Alkyl groups are somehow visible in the range of 3000–2850 cm^{-1}, less contributing to the spectrum in comparison with the original sample and the unreacted solid. Moreover, the presence of esters (~1850 cm^{-1}) and aldehyde functions (~2700 cm^{-1}) are also possible [52,85]. Carboxyl, esters, aromatic esters and ketones C═O functionalities could appear between 1600 and 1800 cm^{-1}, thus all are feasible and not easily discriminated by the bands within this region of the spectrum. The C—O—C and/or sulfonic bands (1360–1100 cm^{-1}) in the oxy-cracked products are less intense compared to the original sample, as occurred with the insoluble solid. One of the most important features of the oxy-cracked sample is the broad-band spanning from about 2300–2800 cm^{-1}; this can be a sign of important contribution of $—CO_3$ (carbonates) to the sample which was isolated under basic conditions thus allowing for this possibility.

From the FTIR results, it could be concluded that the oxidized organic functional groups such as hydroxyl (—OH), carboxylic salts ($O═C—O^-$), carboxylic acids ($R\text{-}CO_2H$) and minor amounts of aldehyde/esters are formed during the oxy-cracking reaction. The functionalities identified by IR spectra of oxy-cracked petcoke are in accordance with the compounds found using XPS and NMR techniques as will be discussed in the next sections.

3.3.2. ^1H NMR analysis of the oxy-cracked petcoke

Nuclear magnetic resonance (NMR) spectroscopy is a very useful technique for identifying and analyzing organic compounds, and it is based on the magnetic properties of atomic nuclei. NMR analysis of oxy-cracked product was performed on a Bruker CFI 600 MHz spectrometer

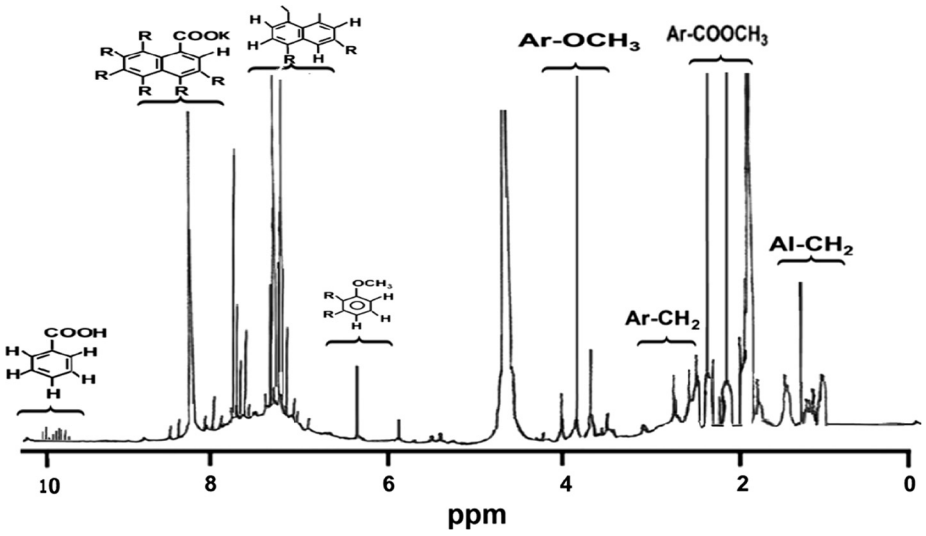

Fig. 11. ^{1}H NMR spectra for oxy-cracked petcoke ran with D_2O solvent. Signal frequencies for typical chemical structures appended.

by dissolving the sample in deuterated water. The ^{1}H NMR spectrum of the oxy-cracked sample produced at 230 °C and 2 h reaction time is shown in Fig. 11. The NMR spectrum indicates that the oxy-cracked sample contains a significant quantity of aliphatic groups with chemical shifts in the range of 0–3 ppm. Methylene moieties (1.8 ppm) and methylenes bonded to the aromatic groups (2–2.7 ppm) can be present in the oxy-cracked sample as also confirmed by the FTIR results [68,86]. However, terminal methyl groups (at about 0.8 ppm) are not detectable as important signals in the oxy-cracked petcoke.

Moreover, the presence of the oxygenated functional groups such as alkoxy groups (probably methoxy, based on the sharp signals determined) are observed in the 3.7–4 ppm region. This is a strong indication, again in agreement with the FTIR and XPS results, that the oxy-cracked products are incorporated with oxygen producing typical oxygenated hydrocarbon compounds like ethers, acids and their salts. On the other hand, aromatic protons span chemical shifts in the range 6–9 ppm. These compounds could be diaromatic carboxylate salts molecules as assigned in the strong signal appearing around 8.5 ppm and methoxy-phenol type molecules (6.5 ppm) as well. The presence of carboxyl groups from carboxylic acids is supported by the small signals appearing around 10 ppm. From the preceding findings, it could be concluded that carboxyl derivatives and oxygenated hydrocarbons produced during oxy-cracking are the most significant fractions solubilized in water. These findings match well with the ones derived from the FTIR spectroscopy and XPS (Section 3.3.3) and are in good agreement with the results obtained by Manasrah et al. [45] and Ashtari et al. [40] for the oxy-cracking of Q-65 and n-C_7 asphaltenes, respectively.

3.3.3. XPS results of petcoke oxy-cracking

As shown previously in the FTIR analysis, Section 3.3.1, the chemical functionalities of petcoke before and after the reaction were identified. Through the XPS analysis, the atomic percentage of the presented elements and group functionalities on the surfaces of original and oxy-cracked products were also determined. Based on the FTIR and the elemental analysis results, the deconvolution of C1s, O1s, N1s and S2p signals along their positions was carried out [67]. Table 4 shows the atomic percentages of the main components, types and quantities of functional groups in both samples (i.e., petcoke after and before reaction). It is clear from the results that the original petcoke is mainly composed of carbon (88.75 at%), and a minor amount of some heteroatoms such as oxygen (8.65 at%), nitrogen (1.05 at%) and sulfur (1.55 at%). However, the oxy-cracked sample showed a higher oxygen percentage (67.70 at%) and much lower carbon (28.60 at%) and sulfur percentage (0.80 at%) compared with the original petcoke sample.

Fig. 12a and b show the deconvoluted C1s spectra of petcoke before and after oxy-cracking. The deconvolution of C1s signals was performed through centering the peaks for different functional groups at specific binding energy levels. It is clearly observed that the distribution of carbon species in the original petcoke was dramatically different than the one corresponding to the oxy-cracked sample. The C1s spectrum of original petcoke (Fig. 12a), contains mainly four bond types (C═C), (C−C), (C−O) and (C═O) set to 283.79 eV, 284.80 eV, 286.34 eV, and 289.21 eV, respectively [67,87]. The abundance of the 283.79 eV band (C═C) evidences that the petcoke sample contained a high amount of aromatic compounds and lower amount of oxygenated functionalities, as revealed by the FTIR and NMR analyses as well. However, the C1s spectrum of oxy-cracked sample (Fig. 12b) shows the presence of similar signals as in the original petcoke with completely different intensities. Hence, the signal intensity attributed to the aromatic bonds (C═C) is much decreased, while the abundance of oxygenated functions (O−C═O) was found very important. Fig. 13 (oxygenates XPS) confirms the presence of carboxyl functions, as well as new C−OH, formed functionalities. The signal at 530.32 eV in both samples (i.e., original and oxy-cracked) attributed to the oxygen in C−O/O−C═O bonds which is higher by almost three times in oxy-cracked sample compared to the original petcoke. Interestingly enough, a distinctive signal at 532.77 eV in oxy-cracked sample (Fig. 13b) is observed and attributed to oxygen in alcoholic groups (C−OH). This can be explained by the high degree of oxidation in petcoke during the oxy-cracking reaction. These findings are indeed in a good agreement with the results obtained from the FTIR and NMR analyses (Figs. 10 and 11).

On the other hand, the presence of heteroatoms such as nitrogen and sulfur are evidenced in Figs. 14 and 15, respectively. Fig. 14a and b show the N1s spectra for both samples. The spectra indicate the presence of pyridines (C−N═C) at 397.89 eV, which are naturally occurring. Similarly, the S2p doublet of petcoke was observed at 163.68 and 164.28 eV (Fig. 15a). It indicated the presence of sulfur-containing functional groups such as thiophenics, sulphonic species (166.7 eV) and low contribution of sulfates (168 eV). Interestingly, lower contribution from thiophenics was observed in the oxy-cracked sample (Fig. 15b) which is indicated by the relatively lower intensity of the S2p doublet. However, the sulphate contribution was found to be higher and particularly sulphonic species (166.7 eV) were found much more important in the oxy-cracked sample. Thus, it can be concluded that the sulfur compounds could exist in oxy-cracked sample, however, with a low contribution (25% reduction) as will be shown in the next section.

3.4. Sulfur and metal analysis

The content of sulfur and metals strongly depend on the nature and

Table 4
Signal fitting for high-resolution spectra of species in original and oxy-cracked petcoke.

	Before Reaction			After Reaction		
	Atomic Conc. (%)	Bond assignment	Bond Conc. (%)	Atomic Conc. (%)	Bond assignment	Bond Conc. (%)
		C=C	70.66		C=C	16.18
		C–C/C–H	16.05		C–C/C–H	43.09
		C–O	8.91		C–O	
C1s	88.75	C=O	2.48	28.60	O-C=O	40.5
		C-O	8.91		C-O, O=C	
		C=O	2.48		OH	
					C=O	40.5
O1s	8.65			67.70	C-OH	
		C-N=C	1.02		C-N=C	0.05
N1s	1.05			2.90		
		C-S-C	0.90		C-S-C	---
S2p	1.55	S-O		0.80	S-O	

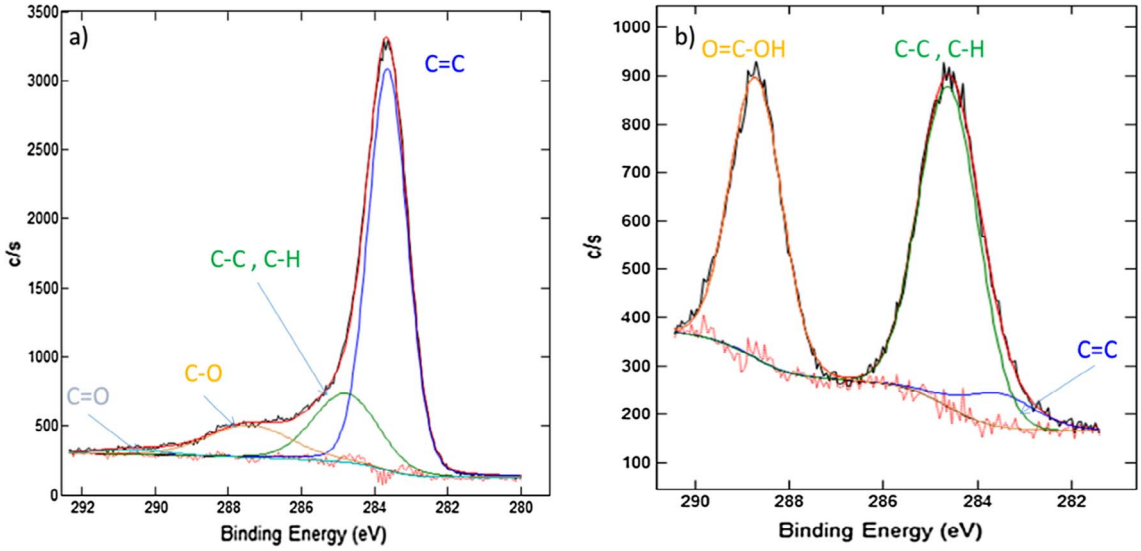

Fig. 12. High-resolution XPS spectra of the deconvoluted C1s peak (a) before reaction, (b) after reaction.

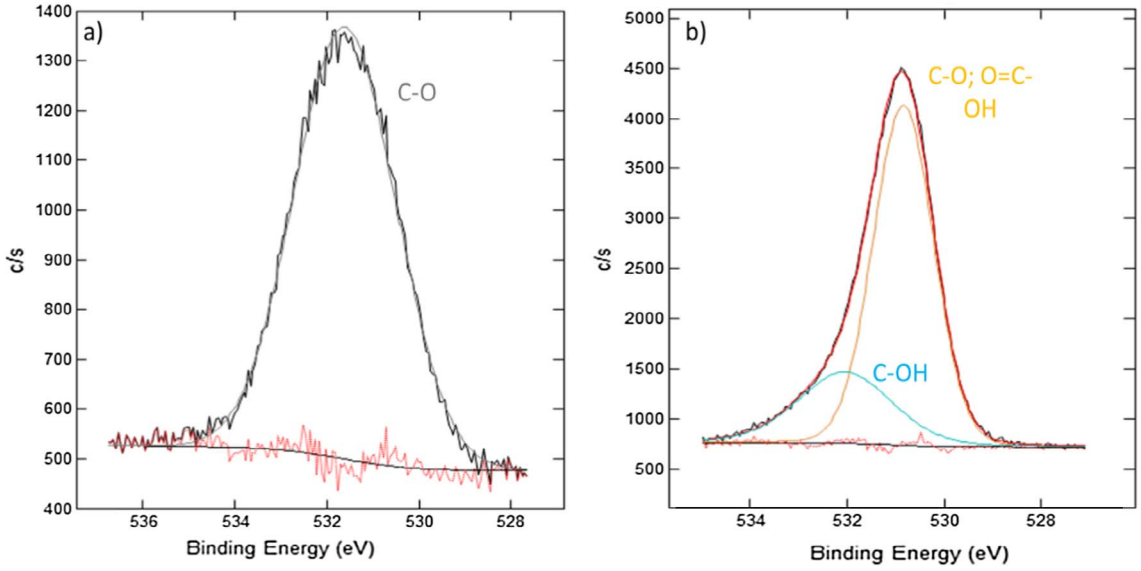

Fig. 13. High-resolution XPS spectra of the deconvoluted O1s peak (a) before reaction, (b) after reaction.

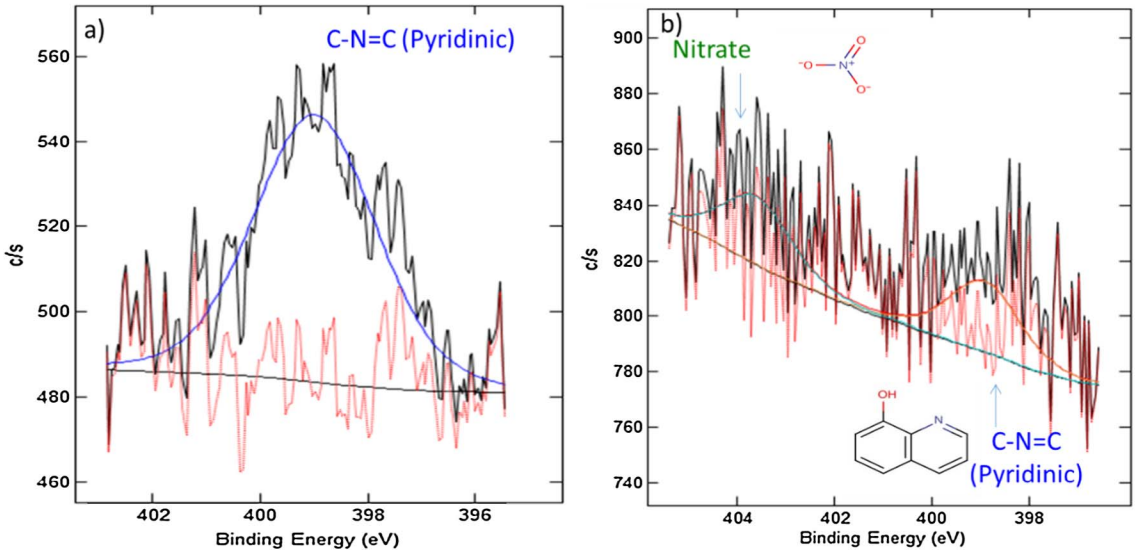

Fig. 14. High-resolution XPS spectra of the deconvoluted N1s peak (a) before reaction, (b) after reaction.

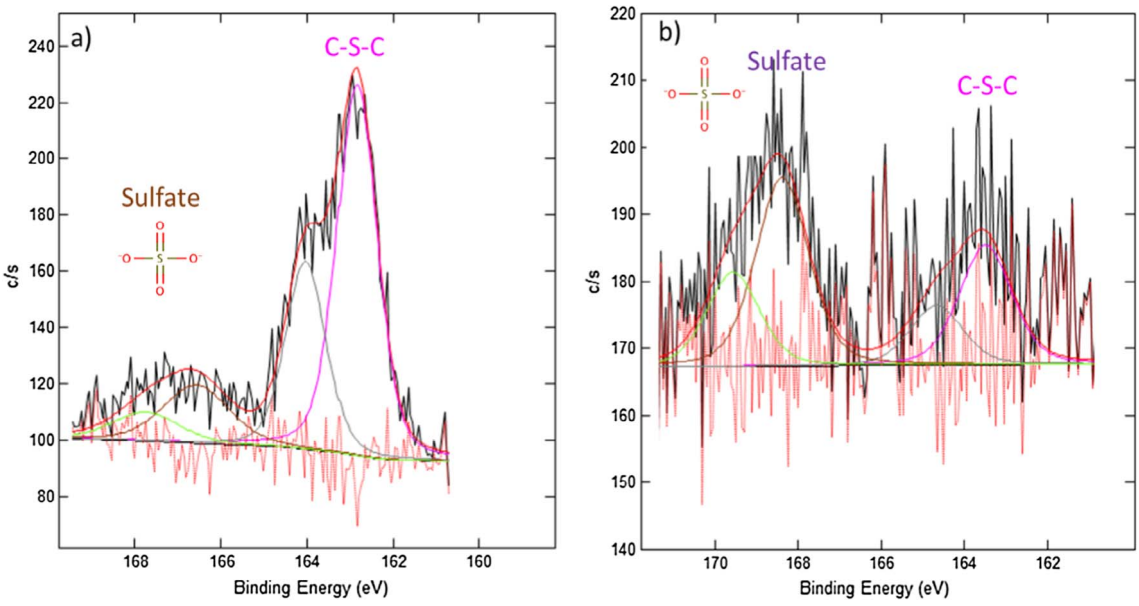

Fig. 15. High-resolution XPS spectra of the deconvoluted S2p peak (a) before reaction, (b) after reaction.

Table 5
Elemental content in the virgin, oxy-cracked and residue petcoke at temperature 230 °C, pressure 750 psi and time 2 h.

Elements	Original (mg)	Residual (mg)	Liquid (mg)	Total mass proportion %
C	844.750	40.710	747.350	95.89
H	38.100	2.280	33.850	94.82
N	15.500	2.850	6.650	93.54
S	44.600	11.740	27.450	87.87
V	0.785	0.114	0.576	87.89
Ni	0.255	0.097	0.203	117.72
Fe	0.568	1.088	0.018	194.78
Mo	0.012	0.011	0.004	125.00
Co	0.151	0.044	0.018	41.10
Total	944.721	85.890	816.677	95.537

the coking process of crude oil, which can be found as organic and inorganic compounds [21,88]. The sulfur compounds, for example, one of the most significant impurities in petcoke, could be attached to the carbon skeleton as thiophenes or to aromatic naphthenic molecules or between the aromatic sheets [21,89]. On the other hand, the presence of metals, mainly nickel and vanadium, could occur as metal chelates or porphyrines as in the asphaltenes [90,91]. However, other metals are not chemically bonded but intercalated in the petcoke structure, as mineral salts normally found as part of ashes [92,93].

In this set of experiments, the element analysis of petcoke was taken into consideration during the oxy-cracking reaction to investigate the ability of this process to demineralize the petcoke. Table 5 shows the elemental analysis for the original petcoke sample (1000 mg), water solubilized products (oxy-cracked sample) and the remaining solids (residue) after the reaction that was carried out at 230 °C for 2 h. Worth to mention that these results were obtained at high reaction conversion, which means that the whole sample of petcoke was targeted to be solubilized in water. As seen in the table, more carbon, hydrogen and nitrogen can be found in the liquid phase compared with residual solid. These findings indicate that 95% of petcoke being oxy-cracked and solubilized in water as discussed early in Section 3.1. Moreover, the primary heteroatoms and metals present in the original petcoke sample

are sulfur and metals like vanadium, nickel, iron, cobalt and molybdenum. The produced hydrocarbons in the liquid phase were determined to contain some amounts of sulfur and metals. However, more iron, nickel, cobalt and molybdenum content can be observed in the residual solid compared with the liquid phase (oxy-cracked products). In addition, more iron and nickel were found in the residual solid compared with the original petcoke. The reason behind that is because of the acidic medium formed during the oxy-cracking reaction which caused corrosion to the reactor wall and impeller, thus metals would be leached out and increase their content in the residue. Interestingly, around 26% of sulfur remained in the residual solids, presumably as highly-fused sulfur aromatic rings and possible coprecipitated sulfates. It can be concluded from these findings that the non-solubilized solids (residue) contain a higher amount of metals compared with the oxy-cracked petcoke (solubilized). These findings suggest that the oxy-cracking process could be a useful technique for petcoke demineralization and desulfurization. Details and further investigation on the operating conditions for the demineralization and desulfurization of petcoke are beyond the scope of this study and will be addressed in a future publication.

4. Conclusion

A new approach for petcoke conversion into valuable products was explored in this study by using oxy-cracking reaction which is operating at mild temperature and pressure in an aqueous alkaline medium. The reaction conditions were experimentally investigated in a batch reactor to optimize the highest conversion and selectivity to water-solubilized products with minimal amount of CO_2 emission, where the optimal temperature and time were 230 °C and 2 h, respectively. The reaction kinetics was established at the residence times ranged between 0 and 2 h and different reaction temperatures 200, 215, and 230 °C. The kinetics results showed that the petcoke is oxy-cracked simultaneously into water-soluble species and CO_2, with the consecutive reaction of soluble species into CO_2. The concentration of the oxy-cracked petcoke in the liquid phase was measured as a lumped TOC, while CO_2 was determined in gas products at the end of reaction using gas chromatography (GC) and inorganic carbon (IC). The oxygenated hydrocarbons (desired products) and the residual solids were characterized using FTIR, NMR and XPS techniques. The results showed that the main species solubilized in water were oxygenated hydrocarbons compounds and some organic acid such as carboxylic and sulfonic acids and their salts. The residual solids remaining after the reaction showed structures and functional groups similar to the original petcoke. Interestingly, most of the metals contents were found in the residual petcoke compared with the metals in the liquid phase. Therefore, the oxy-cracking technique can be considered as a new feasible process for conversion and demineralization/desulfurization of petroleum coke.

Acknowledgments

The authors are grateful to the Natural Sciences and Engineering Research Council of Canada (NSERC), the Department of Chemical and Petroleum Engineering at the Schulich School of Engineering at the University of Calgary. A special thank to Dr. Maha AbuHafeetha Nassar for her help in drawing the schematic diagram of the experimental setup. Also, the authors acknowledge Dr. M. Josefina Perez-Zurita and Marianna Trujillo for helping in the XPS and NMR analyses.

References

[1] Speight JG. New approaches to hydroprocessing. Catal Today 2004;98(1):55–60.
[2] Hsu CS, Robinson P. Practical advances in petroleum processing. Springer Science & Business Media; 2007.
[3] Furimsky E. Characterization of cokes from fluid/flexi-coking of heavy feeds. Fuel Process Technol 2000;67(3):205–30.
[4] Furimsky E. Gasification of oil sand coke: review. Fuel Process Technol 1998;56(3):263–90.
[5] Zubot W, MacKinnon MD, Chelme-Ayala P, Smith DW, El-Din MG. Petroleum coke adsorption as a water management option for oil sands process-affected water. Sci Total Environ 2012;427:364–72.
[6] Rana MS, Samano V, Ancheyta J, Diaz J. A review of recent advances on process technologies for upgrading of heavy oils and residua. Fuel 2007;86(9):1216–31.
[7] Dutta RP, McCaffrey WC, Gray MR, Muehlenbachs K. Thermal cracking of Athabasca bitumen: influence of steam on reaction chemistry. Energy Fuels 2000;14(3):671–6.
[8] Yoon SJ, Choi Y-C, Lee S-H, Lee J-G. Thermogravimetric study of coal and petroleum coke for co-gasification. Korean J Chem Eng 2007;24(3):512–7.
[9] C.E.f.i. Peace, Managing China's petcoke problem; 2015. http://carnegieendowment.org/files/petcoke.pdf. (Accessed October 2016).
[10] N.R. Canada, Oil Sands: A strategic resource for Canada, North America and the global market; 2013. http://www.nrcan.gc.ca/sites/www.nrcan.gc.ca/files/energy/pdf/eneene/pubpub/pdf/OS-brochure-eng.pdf. (Accessed 10 March 2017).
[11] EPA, U.S. Environmental Protection Agency; 2011. http://www.epa.gov/p2/pubs/p2policy/definitions.htm. (Accessed January 2016).
[12] Ityokumbul MT. Experimental evaluation of molten caustic leaching of an oil sand coke residue. Can J Chem Eng 1994;72(2):370–4.
[13] Jang H, Etsell TH. Morphological and mineralogical characterization of oil sands fly ash. Energy Fuels 2005;19(5):2121–8.
[14] Pourrezaei P, Alpatova A, Chelme-Ayala P, Perez-Estrada L, Jensen-Fontaine M, Le X, et al. Impact of petroleum coke characteristics on the adsorption of the organic fractions from oil sands process-affected water. Int J Environ Sci Technol 2014;11(7):2037–50.
[15] Hill JM, Karimi A, Malekshahian M. Characterization, gasification, activation, and potential uses for the millions of tonnes of petroleum coke produced in Canada each year. Can J Chem Eng 2014;92(9):1618–26.
[16] Fedorak PM, Coy DL. Oil sands cokes affect microbial activities. Fuel 2006;85(12):1642–51.
[17] Wang J, Anthony EJ, Abanades JC. Clean and efficient use of petroleum coke for combustion and power generation. Fuel 2004;83(10):1341–8.
[18] Ellis PJ, Paul CA. Tutorial: Petroleum coke calcining and uses of calcined petroleum coke. American Institute of Chemical Engineers; 2000.
[19] Caruso JA, Zhang K, Schroeck NJ, McCoy B, McElmurry SP. Petroleum coke in the urban environment: a review of potential health effects. Int J Environ Res Public Health 2015;12(6):6218–31.
[20] Farago FJ, Retallack DG, Sood RR. Calcination of coke, US Patent 4,022,569; 1977.
[21] Al-Haj-Ibrahim H, Morsi BI. Desulfurization of petroleum coke: a review. Ind Eng Chem Res 1992;31(8):1835–40.
[22] Edwards L, Vogt F, Robinette M, Love R, Ross A, McClung M, Roush R, Morgan W. Use of shot coke as an anode raw material, Essential readings in light metals: electrode technology for aluminum production 2013;4:36–41.
[23] Dunbar R, Eng P. Canada's oil sands-a world-scale hydrocarbon resource, strategy. West Inc; 2007.
[24] Sarkar B. Adsorption of single-ring model naphthenic acid from oil sands tailings pond water using petroleum coke-derived activated carbon. University of Toronto; 2013.
[25] Hall E, Tollefson E, George Z, Schneider L. Upgrading of delayed and fluid cokes from oil sand by desulfurization. Can J Chem Eng 1982;60(3):418–24.
[26] Lee SH, Choi CS. Chemical activation of high sulfur petroleum cokes by alkali metal compounds. Fuel Process Technol 2000;64(1):141–53.
[27] Berguerand N, Lyngfelt A. The use of petroleum coke as fuel in a 10 kW_{th} chemical-looping combustor. Int J Greenhouse Gas Control 2008;2(2):169–79.
[28] Small C. Activation of delayed and fluid petroleum coke for the adsorption and removal of naphthenic acids from oil sands tailings pond water. University of Alberta; 2011.
[29] Li X, Zhang Q, Tang L, Lu P, Sun F, Li L. Catalytic ozonation of p-chlorobenzoic acid by activated carbon and nickel supported activated carbon prepared from petroleum coke. J Hazard Mater 2009;163(1):115–20.
[30] Zubot WA. Removal of naphthenic acids from oil sands process water using petroleum coke. University of Alberta; 2011.
[31] Morris EA. Modification of carbonaceous materials with sulfur and its impact on mercury capture and sorbent regeneration. University of Toronto; 2012.
[32] Awoyemi A. Understanding the adsorption of polycyclic aromatic hydrocarbons from aqueous phase onto activated carbon. University of Toronto; 2011.
[33] Hethnawi A, Nassar NN, Manasrah AD, Vitale G. Polyethylenimine-functionalized pyroxene nanoparticles embedded on Diatomite for adsorptive removal of dye from textile wastewater in a fixed-bed column. Chem Eng J 2017;320:389–404.
[34] Stavropoulos G, Zabaniotou A. Minimizing activated carbons production cost. Fuel Process Technol 2009;90(7):952–7.
[35] Bandosz TJ. Activated carbon surfaces in environmental remediation. New York USA: Academic press; 2006.
[36] Nassar NN, Hassan A, Pereira-Almao P. Application of nanotechnology for heavy oil upgrading: catalytic steam gasification/cracking of asphaltenes. Energy Fuels 2011;25(4):1566–70.
[37] González A, Moreno N, Navia R. CO_2 carbonation under aqueous conditions using petroleum coke combustion fly ash. Chemosphere 2014;117:139–43.
[38] Nemanova V, Abedini A, Liliedahl T, Engvall K. Co-gasification of petroleum coke and biomass. Fuel 2014;117:870–5.
[39] Solutions AI-EaE. Executive Summary; 2017. http://eipa.alberta.ca/. (Accessed March 2017).
[40] Ashtari M, Carbognani Ortega L, Lopez-Linares F, Eldood A, Pereira-Almao P. New pathways for asphaltenes upgrading using the oxy-cracking process. Energy Fuels 2016;30(6):4596–608.

[41] Ashtari M. New pathways for asphaltenes upgrading via oxy-cracking in liquid phase. University of Calgary; 2016.
[42] Smith Moreno-Arciniegas L, Rodríguez-Corredor F-E, Afanador-Rey L-E, Grosso-Vargas J-L. Syngas obtainment from the gasification of asphaltenes of the San Fernando crude oil. CT&F-Ciencia Tecnol Futuro 2009;3(5):189–202.
[43] Haghighat P, Carbognani Ortega L, Pereira-Almao P. Experimental study on catalytic hydroprocessing of solubilized asphaltene in water: a proof of concept to upgrade asphaltene in the aqueous phase. Energy Fuels 2016;30(4):2904–18.
[44] Haghighat P. Processing of solubilized asphaltene in aqueous media. University of Calgary; 2016.
[45] Manasrah AD, El-Qanni A, Badran I, Carbognani L, Perez-Zurita MJ, Nassar NN. Experimental and theoretical studies on oxy-cracking of Quinolin-65 as a model molecule for residual feedstocks. React Chem Eng 2017;2:703–19.
[46] Moschopedis S, Speight J. Oxidative degradation of Athabasca asphaltenes. Fuel 1971;50(2):211–7.
[47] Platonov V, Kudrya A, Proskuryakov S. Ozonolysis of asphaltenes from semicoking tar of G17 coal. Russ J Appl Chem 2003;76(1):148–52.
[48] Moschopedis SE. Sulfomethylation of humic acids, lignites, and coals and products thereof, US Patent 3,352,902; 1967.
[49] Moschopedis SE, Speight JG. Influence of metal salts on bitumen oxidation. Fuel 1978;57(4):235–40.
[50] Escobar G, Patiño P, Acevedo S, Escobar O, Ranaudo MA, Pereira JC. Interfacial properties of the products of ozonolysis of Hamaca crude oil. Pet Sci Technol 2001;19(1–2):107–18.
[51] Marei NN, Nassar NN, Hmoudah M, El-Qanni A, Vitale G, Hassan A. Nanosize effects of NiO nanosorbcats on adsorption and catalytic thermo-oxidative decomposition of vacuum residue asphaltenes. Can J Chem Eng 2017.
[52] Ashtari M, Carbognani L, Pereira-Almao P. Asphaltenes aqueous conversion to humic and fulvic analogs via oxy-cracking. Energy Fuels 2016;30(7):5470–82.
[53] Haghighat P, Carbognani Ortega L, Pereira-Almao P. Kinetic study of preoxidized asphaltene hydroprocessing in aqueous phase. Energy Fuels 2016;30(7):5617–29.
[54] Li L, Chen P, Gloyna EF. Generalized kinetic model for wet oxidation of organic compounds. AIChE J 1991;37(11):1687–97.
[55] Estrade-Szwarckopf H. XPS photoemission in carbonaceous materials: a “defect” peak beside the graphitic asymmetric peak. Carbon 2004;42(8):1713–21.
[56] Zhang Q, Chuang KT. Lumped kinetic model for catalytic wet oxidation of organic compounds in industrial wastewater. AIChE J 1999;45(1):145–50.
[57] Marei NN, Nassar NN, Vitale G, Hassan A, Zurita MJP. Effects of the size of NiO nanoparticles on the catalytic oxidation of Quinolin-65 as an asphaltene model compound. Fuel 2017;207:423–37.
[58] Seshadri KS, Albaugh EW, Bacha JD. Characterization of needle coke feedstocks by magnetic resonance spectroscopy. Fuel 1982;61(4):336–40.
[59] Sarkar A, Kocaefe D, Kocaefe Y, Bhattacharyay D, Morais B, Pouliot M. Characterization of petroleum coke and butts used in anode manufacturing in aluminum industry. In: Materials science and technology conference and exhibition 2013, MS and T 2013; 2014.
[60] Brouwer EB, Moudrakovski I, Chung KH, Pleizier G, Ripmeester JA, Deslandes Y. Magnetic resonance microimaging of petroleum coke. Energy Fuels 1999;13(5):1109–10.
[61] Rivas J, Kolaczkowski ST, Beltran FJ, McLurgh DB. Degradation of maleic acid in a wet air oxidation environment in the presence and absence of a platinum catalyst. Appl Catal B 1999;22(4):279–91.
[62] Merchant K. Studies of heterogeneous reactions PhD thesis India: Department of Chemical Technology, University of Bombay; 1992
[63] Shende RV, Levec J. Kinetics of wet oxidation of propionic and 3-hydroxypropionic acids. Ind Eng Chem Res 1999;38(7):2557–63.
[64] Rodriguez N, Marsh H, Heintz E, Sherwood R, Baker R. Oxidation studies of various petroleum cokes. Carbon 1987;25(5):629–35.
[65] Badran I, Nassar NN, Marei NN, Hassan A. Theoretical and thermogravimetric study on the thermo-oxidative decomposition of Quinolin-65 as an asphaltene model molecule. RSC Adv 2016;6(59):54418–30.
[66] Menéndez J, Pis J, Alvarez R, Barriocanal C, Fuente E, Diez M. Characterization of petroleum coke as an additive in metallurgical cokemaking. Modification of thermoplastic properties of coal. Energy Fuels 1996;10(6):1262–8.
[67] Sarkar A, Kocaefe D, Kocaefe Y, Bhattacharyay D, Sarkar D, Morais B. Effect of crystallinity on the wettability of petroleum coke by coal tar pitch. Energy Fuels 2016;30(4):3549–58.
[68] Castro AT. NMR and FTIR characterization of petroleum residues: structural parameters and correlations. J Braz Chem Soc 2006;17(6):1181–5.
[69] Lin S, Ho S. Treatment of high-strength industrial wastewater by wet air oxidation a case study. Waste Manage (Oxford) 1997;17(1):71–8.
[70] Parvas M, Haghighi M, Allahyari S. Catalytic wet air oxidation of phenol over ultrasound-assisted synthesized Ni/CeO_2–ZrO_2 nanocatalyst used in wastewater treatment. Arab J Chem 2014.
[71] Portela J, Nebot E, de la Ossa EM. Kinetic comparison between subcritical and supercritical water oxidation of phenol. Chem Eng J 2001;81(1):287–99.
[72] Abussaud BA, Ulkem N, Berk D, Kubes GJ. Wet air oxidation of benzene. Ind Eng Chem Res 2008;47(13):4325–31.
[73] Suppes G, Roy S, Ruckman J. Impact of common salts on oxidation of alcohols and chlorinated hydrocarbons. AIChE J 2001;47(7):1623–31.
[74] Headley JV, Peru KM, Mcmartin DW, Winkler M. Determination of dissolved naphthenic acids in natural waters by using negative-ion electrospray mass spectrometry. J AOAC Int 2002;85(1):182–7.
[75] Patil PT, Armbruster U, Richter M, Martin A. Heterogeneously catalyzed hydroprocessing of organosolv lignin in sub-and supercritical solvents. Energy Fuels 2011;25(10):4713–22.
[76] Konnerth H, Zhang J, Ma D, Prechtl MH, Yan N. Base promoted hydrogenolysis of lignin model compounds and organosolv lignin over metal catalysts in water. Chem Eng Sci 2015;123:155–63.
[77] Chunlan L, Shaoping X, Yixiong G, Shuqin L, Changhou L. Effect of pre-carbonization of petroleum cokes on chemical activation process with KOH. Carbon 2005;43(11):2295–301.
[78] Akhter M, Keifer J, Chughtai A, Smith D. The absorption band at 1590 cm − 1 in the infrared spectrum of carbons. Carbon 1985;23(5):589–91.
[79] Meldrum BJ, Rochester CH. In situ infrared study of the surface oxidation of activated carbon in oxygen and carbon dioxide. J Chem Soc, Faraday Trans 1990;86(5):861–5.
[80] Manasrah AD, Laoui T, Zaidi SJ, Atieh MA. Effect of PEG functionalized carbon nanotubes on the enhancement of thermal and physical properties of nanofluids. Exp Therm Fluid Sci 2017;84:231–41.
[81] Pruski M, Gerstein B, Michel D. NMR of petroleum cokes II: studies by high resolution solid state NMR of 1H and 13C. Carbon 1994;32(1):41–9.
[82] Michel D, Pruski M, Gerstein B. NMR of petroleum cokes I: relaxation studies and quantitative analysis of hydrogen by magnetic resonance. Carbon 1994;32(1):31–40.
[83] Suriyapraphadilok U. Characterization of coal-and petroleum-derived binder pitches and the interaction of pitch/coke mixtures in pre-baked carbon anodes, ProQuest2008.
[84] Hethnawi A, Manasrah AD, Vitale G, Nassar NN. Fixed-bed column studies of total organic carbon removal from industrial wastewater by use of diatomite decorated with polyethylenimine-functionalized pyroxene nanoparticles. J Colloid Interface Sci 2017.
[85] Claine Petersen J. A dual, sequential mechanism for the oxidation of petroleum asphalts. Pet Sci Technol 1998;16(9–10):1023–59.
[86] Grasso D, Chin Y-P, Weber WJ. Structural and behavioral characteristics of a commercial humic acid and natural dissolved aquatic organic matter. Chemosphere 1990;21(10–11):1181–97.
[87] Huang X, Kocaefe D, Kocaefe Y, Bhattacharyay D. Wettability of bio-coke by coal tar pitch for its use in carbon anodes. Colloids Surf, A 2016;490:133–44.
[88] Andrews A, Lattanzio RK. Petroleum coke: industry and environmental issues, congressional research service; 2014.
[89] Meyers RA. Coal desulfurization. New York: Marcel Dekker Inc.; 1977.
[90] Shlewit H, Alibrahim M. Extraction of sulfur and vanadium from petroleum coke by means of salt-roasting treatment. Fuel 2006;85(5):878–80.
[91] Alvarado J, Alvarez M, Cristiano AR, Marcó L. Extraction of vanadium from petroleum coke samples by means of microwave wet acid digestion. Fuel 1990;69(1):128–30.
[92] Agarwal P, Sharma D. Studies on the desulfurization of petroleum coke by organorefining and other chemical and biochemical techniques under milder ambient pressure conditions. Pet Sci Technol 2011;29(14):1482–93.
[93] Queneau P, Hogsett R, Beckstead L, Barchers D. Processing of petroleum coke for recovery of vanadium and nickel. Hydrometallurgy 1989;22(1–2):3–24.